

## Slow fluctuations in recurrent networks of spiking neurons

Stefan Wieland,<sup>1,2</sup> Davide Bernardi,<sup>1,2</sup> Tilo Schwalger,<sup>3</sup> and Benjamin Lindner<sup>1,2</sup>

<sup>1</sup>*Bernstein Center for Computational Neuroscience Berlin, Philippstrasse 13, Haus 2, 10115 Berlin, Germany*

<sup>2</sup>*Physics Department of Humboldt University Berlin, Newtonstrasse 15, 12489 Berlin, Germany*

<sup>3</sup>*School of Computer and Communication Sciences and School of Life Sciences, Brain Mind Institute,*

*École Polytechnique Fédérale de Lausanne, Station 15, 1015 Lausanne EPFL, Switzerland*

(Received 24 July 2015; published 5 October 2015)

Networks of fast nonlinear elements may display slow fluctuations if interactions are strong. We find a transition in the long-term variability of a sparse recurrent network of perfect integrate-and-fire neurons at which the Fano factor switches from zero to infinity and the correlation time is minimized. This corresponds to a bifurcation in a linear map arising from the self-consistency of temporal input and output statistics. More realistic neural dynamics with a leak current and refractory period lead to smoothed transitions and modified critical couplings that can be theoretically predicted.

DOI: [10.1103/PhysRevE.92.040901](https://doi.org/10.1103/PhysRevE.92.040901)

PACS number(s): 84.35.+i, 07.05.Mh, 05.40.–a

How can slow fluctuations build up in a network of fast elements? This is a fundamental question for many systems in physics and biology, ranging from spin glasses [1] to systems generating  $1/f$  noise [2]. The problem is particularly appealing in neuroscience because the propensity of neural networks for slow change may endow them with what is reminiscent of short-term memory [3–5] and what is required for a number of cognitive functions [6,7]. That is why slow fluctuations and processes on large time scales in such networks have received attention by physicists since the 1980's [8–11] and continue to be in the focus of current research [12–16].

For recurrent networks of spiking neurons, it is hotly debated what kind of transition is observed when the coupling strength is varied—do such networks show a phase transition (manifest by diverging correlation times) as do networks of rate units [8]? Here, we address this problem via a self-consistency condition for the temporal correlations of the single neuron and validate the results by extensive simulations of a large ( $>10^5$  neurons) and sparse recurrent network. A key insight of our study is that for strong coupling the fluctuations seen as well as generated by a single neuron in the network become strongly *colored*—slow fluctuations are most strongly amplified while high-frequency noise remains limited.

It is clear that this colored-noise problem cannot be solved in the otherwise very successful Fokker-Planck framework [17,18], which assumes white (uncorrelated) Gaussian noise as the effective input to a neuron in the network. Here, we employ a recent theory for the spike statistics of integrate-and-fire (IF) neurons driven by noise with arbitrary temporal correlations [19] in order to predict the critical coupling at which long-range temporal correlations of spiking emerge. We show that around this critical coupling, Fano factors of individual neurons strongly increase and their correlation time attains a pronounced minimum, which is in marked contrast to a maximized correlation time close to a phase transition [8]. The transition becomes a true bifurcation for networks of perfect IF neurons (neglecting leak currents). Its hallmarks are still present for networks that include leak currents and an absolute refractory period.

*Network model.* We consider the classical setup by Brunel [18], a random network of  $N_E$  excitatory and  $N_I$  inhibitory

integrate-and-fire (IF) neurons, all obeying

$$\tau_m \dot{v}_k = -\gamma v_k + R[I_{\text{ext}} + I_{\text{syn},k}(t)], \quad (1)$$

with a membrane time constant of  $\tau_m = 20$  ms. The  $k$ th neuron fires whenever the voltage  $v_k(t)$  reaches  $v_T = 20$  mV and is reset to  $v_R = 10$  mV after a refractory period  $\tau_{\text{ref}}$ . The instances of threshold crossings  $t_{k,i}$  define the spike train,  $x_k(t) = \sum_i \delta(t - t_{k,i})$ , of the  $k$ th neuron. Neurons are coupled by current-based instantaneous synapses, including a transmission delay of  $D = 1.5$  ms,

$$I_{\text{syn},k}(t) = \frac{J\tau_m}{R} \left[ \sum_{j=1}^{C_E} x_{\ell_{k,j}}(t - D) - g \sum_{j=1}^{C_I} x_{\kappa_{k,j}}(t - D) \right]. \quad (2)$$

Here, the excitatory (inhibitory) input spike trains  $x_{\ell_{k,j}}(t)$  [ $x_{\kappa_{k,j}}(t)$ ] belong to  $C_E$  ( $C_I$ ) presynaptic neurons  $\ell_{k,j}$  ( $\kappa_{k,j}$ ), chosen at random from the  $N_E$  ( $N_I$ ) excitatory (inhibitory) neurons of the network. We use a sparse fixed connectivity [18] with  $C_E = 10^3$ ,  $C_I = 250$ . The constant external input is  $RI_{\text{ext}} = 30$  mV (mean-driven regime of the single neurons) and  $g = 4$  (balanced recurrent input from the network), keeping the network in the asynchronous firing regime [18], where cross correlations between neurons are negligible. We focus on the spike-train power spectrum in a time window  $T$ ,  $S_{xx}^T(f) = \langle |\tilde{x}_{k,T}(f)|^2 \rangle / T$ , expressed in terms of the Fourier transform  $\tilde{x}_{k,T} = \int_0^T dt e^{2\pi i f t} [x_k(t) - r_0]$  and the firing rate  $r_0 = \langle x_k(t) \rangle$ , where in simulations  $\langle \cdot \rangle$  is taken as the average over  $10^3$  neurons of the network (and—for the firing rate—also over the time window  $T$ ). In the following,  $S_{xx}(f) = \lim_{T \rightarrow \infty} S_{xx}^T(f)$ . In all network simulations, we set  $N_E/N_I = 4$ . Moreover,  $N_E = 10^5$  and  $T = 100$  s unless explicitly indicated.

*Single-neuron iterative scheme.* Self-consistency in the homogeneous network requires that in the asynchronous state the corresponding single-neuron IF model,

$$\dot{v} = (RI_{\text{ext}} - \gamma v) / \tau_m + J r_0 (C_E - g C_I) + J \sqrt{C_E + g^2 C_I} \eta(t), \quad (3)$$

with the fire-and-reset rule introduced above, has a firing rate  $r_0 = \langle x(t) \rangle$  [determining the drift term in Eq. (3)] and a power

spectrum  $S_{xx}^T(f)$  that is equal to the power spectrum of the noise  $\eta(t)$  in Eq. (3), i.e.,  $S_{xx}^T(f) = S_{\eta\eta}^T(f)$ . Both the rate and spectrum can be approximately determined in a single-neuron simulation scheme of Eq. (3), in which iteratively a single neuron is stimulated over several “generations” with surrogate Gaussian noise, the power spectrum of which matches the previous generation’s spike-train spectrum [20,21]. Formally, we iterate a functional map  $M$  that leads from the rate and spectrum of the  $n$ th generation to those of the  $(n+1)$ th,  $(r_0, S_{xx})_{n+1} = M[(r_0, S_{xx})_n]$ —the fixed point of this map yields the self-consistent solution. We use Eq. (3) for  $10^3$  realizations and iterate over  $10^2$  generations to estimate the firing rate and spike-train power spectrum in a time window  $T$  for a sparse network in the asynchronous state. For both the full network simulations and the iterative scheme, we discard an additional transient of 10 s.

*Network of perfect IF neurons.* Switching off the leak term in Eq. (1),  $\gamma = 0$ , we obtain a network of perfect IF neurons. For simplicity, we set  $\tau_{\text{ref}} = D = 0$  ms. Then, the self-consistent rate is  $r_0 = \tau_m^{-1} R I_{\text{ext}} / [v_T - v_R - J(C_E - gC_I)]$ , which is independent of coupling strength for perfect balance,  $g = C_E/C_I = 4$ . Hence, the functional map  $M$  reduces to one solely for the power spectrum.

For a perfect IF neuron, driven by a weak Gaussian noise with arbitrary temporal correlations, expressions for the spike-train autocorrelation function have recently been derived [19] but are too complicated to solve the functional map analytically for its fixed point  $S_{xx}(f)$ . However, it turns out that at zero frequency, the power spectrum of the output is just determined by the input power spectrum at zero frequency [22]. The corresponding spike-train spectrum at zero frequency is important because it is related to the Fano factor  $F(T) = \langle \Delta N^2(T) \rangle / \langle N(T) \rangle$  [variance over mean of the spike count  $N(T)$ ] via  $S_{xx}^T(0) = r_0 F(T)$ —a small (large) value indicates a weak (strong) long-term variability and, generally, the suppression (enhancement) of slow fluctuation in the spike train. Remarkably, the resulting relation between the input spectrum (or the spectrum of the previous generation) and output spectrum (or the spectrum of the next generation) is linear and not limited to a weak input noise or Gaussian noise statistics:

$$S_{xx,n+1}(0) = \frac{J^2(C_E + g^2C_I)}{(v_T - v_R)^2} S_{xx,n}(0). \quad (4)$$

A bifurcation in the stability of this linear map occurs at

$$J_c = \frac{v_T - v_R}{\sqrt{C_E + g^2C_I}}. \quad (5)$$

For a coupling  $J < J_c$ , the power spectrum at zero frequency will decrease to zero. This limit implies the absence of any long-term variability in the spike trains of weakly coupled perfect IF neurons. In the opposite limit of  $J > J_c$ , the power spectrum in the map Eq. (4) (and the Fano factor) grows without bound.

These expectations are confirmed by spike-train power spectra from both network simulations and the single-neuron iterative scheme, shown in Fig. 1. Because of limitations in network size, number of generations, simulation time step, and time window  $T$  for the Fourier transform, we cannot

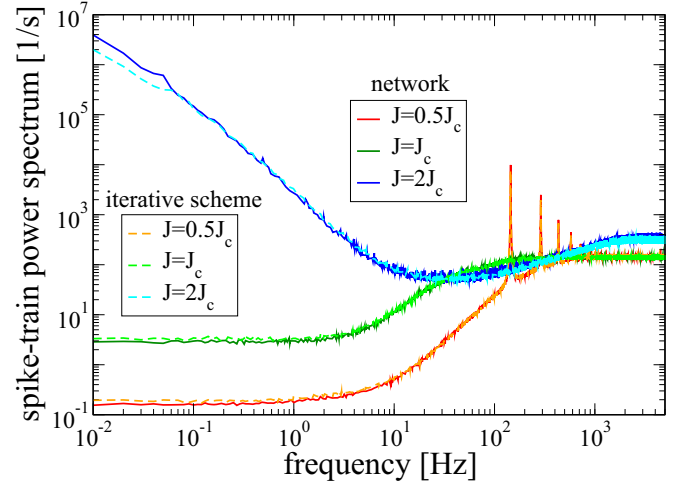


FIG. 1. (Color online) Network of perfect IF neurons: Single-neuron spike-train power spectra from network simulations (solid lines) and from iterative single-neuron simulations (dashed lines) for subcritical, critical, and supercritical synaptic coupling with  $J_c = (\sqrt{2}/10)$  mV  $\approx 0.14$  mV. Firing rates estimated from the same simulations in the three cases are  $r_0 = 145$ , 141, and 352 Hz for  $J = J_c/2$ ,  $J_c$ , and  $2J_c$ , respectively. For longer simulation times and shorter time steps, firing rates in all three cases get closer to the theoretical value of  $r_0 = 150$  Hz.

expect to see the exact asymptotic limits of the map, Eq. (4). What we see instead is a drastic effect of the value of the coupling constant  $J$  (changed by a modest factor of 4) on the power spectra at low frequencies that differ by seven orders of magnitude if we go from subcritical to supercritical coupling strength. This is in line with previous observations of increased low-frequency power in other models in which the coupling strength was varied [23,24]. The spike-train power spectra obtained from the iterative simulations (dashed lines in Fig. 1) are generally close to those determined from network simulations, which supports the above line of reasoning and indicates that neglected features such as correlations among the neurons do not play a significant role.

Remarkably, the zero-frequency limit in the subcritical case is not approached via a completely deterministic spike train (which would have zero power at zero frequency), but by negative correlations of its interspike intervals [25]. Note that  $S_{xx}^T(0)$  as obtained in our simulations is small but not exactly zero because of the finite time step of  $\Delta t = 0.1$  ms; reducing  $\Delta t$  leads to a further reduction of  $S_{xx}^T(0)$  (not shown).

At critical coupling, the power spectrum looks similar to spectra that have been measured in cortical cells [26]: There is reduced power at low frequencies and a small hump close to the firing rate of the cell. In the supercritical case at  $J = 2J_c$ , the power spectrum shows a pronounced  $1/f^\alpha$  (with  $\alpha \approx 1.8$ ) divergence, in accordance with the divergence of the map in this case.

Two characteristics can be extracted from the power spectra, the Fano factor and the correlation time. By taking  $S_{xx}^T(0)/r_0$ , we obtain the Fano factor  $F(T)$ , i.e., a measure of the spike train’s long-term variability in the time window of the simulation.

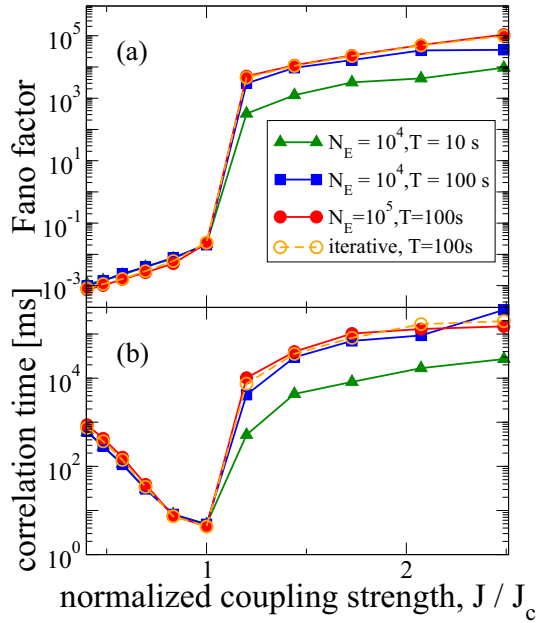


FIG. 2. (Color online) Network of perfect IF neurons: (a) Fano factor and (b) correlation time as functions of normalized synaptic coupling strength (here,  $J_c \approx 0.14$  mV) for different values of network size and time window from network simulations (solid lines) and iterative scheme (dashed lines).

Further, given the spike train's correlation function  $c(\tau) = \langle x(t)x(t+\tau) \rangle - \langle x \rangle^2$ , following Ref. [27] we consider its continuous part  $\hat{c}(\tau) = c(\tau) - r_0\delta(\tau)$  and define the correlation time as the integral over the normalized square of this function,

$$\tau_c = \int_{-\infty}^{+\infty} d\tau \left[ \frac{\hat{c}(\tau)}{\hat{c}(0)} \right]^2 = \int_{-\infty}^{\infty} df \frac{(S_{xx}(f) - r_0)^2}{r_0^4}. \quad (6)$$

In the last step, we used the Parseval theorem to express  $\tau_c$  by the power spectrum.

When the coupling strength is varied, the Fano factor [Fig. 2(a)] shows a sharp transition at  $J \simeq J_c$ , separating exponentially small values ( $J < J_c$ ) from exponentially large values ( $J > J_c$ ) with an overall variation over eight orders of magnitude if  $J$  is varied by less than a factor of ten. Increasing the time window by a factor of ten leads to a similar increase of the Fano factor for  $J > J_c$ . In contrast, an increase of the network size (from  $N_E = 10^4$  to  $N_E = 10^5$ ) has only a little effect on the Fano factor curve.

The correlation time shows at the first glance a surprising *minimum* around the critical value  $J \approx J_c$ , which stands in marked contrast to the *maximum* predicted in the rate network with all-to-all coupling by Sompolinsky *et al.* [8]. From our simple map, Eq. (4), we would expect that the divergence is more pronounced for stronger coupling and so it is plausible that  $\tau_c$  grows with  $J$  once we are beyond the critical coupling. In the other limit, for  $J \rightarrow 0$ , neurons fire asynchronously but perfectly regularly and thus we expect  $\tau_c \rightarrow \infty$  in this limit as well.

*Network of leaky IF neurons.* How much of the transition effect remains if we switch on a finite leak term ( $\gamma > 0$ ) in Eq. (1) and take into account an absolute refractory period

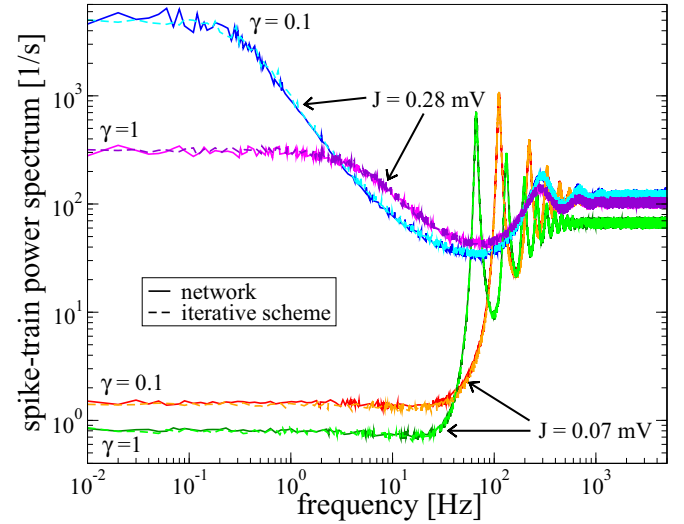


FIG. 3. (Color online) Network of leaky IF neurons: Single-neuron spike-train power spectra from network simulations (solid lines) and from the iterative scheme (dashed lines) for weak and strong synaptic coupling and two values of the leak parameter  $\gamma$  as indicated.

and a finite transmission delay  $D = 1.5$  ms? In numerical simulations of large networks of leaky IF (LIF) neurons we find that the (supercritical) divergence or (subcritical) vanishing of the spectrum at zero frequency is smoothed to finite values (Fig. 3). However, these values still differ by orders of magnitude for the Fano factor [Fig. 4(a)]; networks of leaky IF neurons still show a remarkably deep minimum of the spike train's correlation time as a function of the

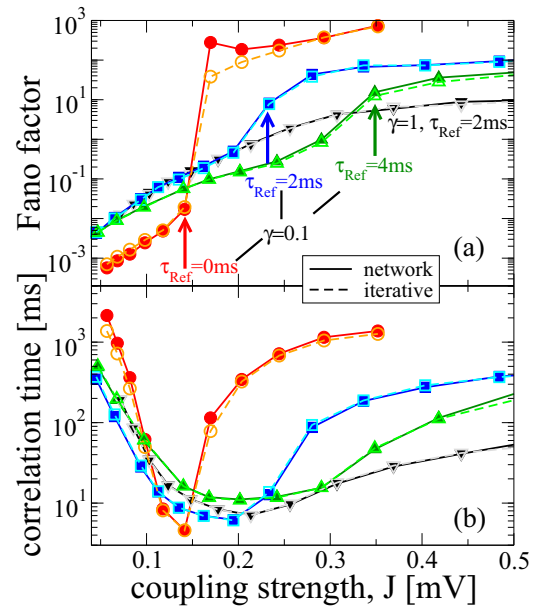


FIG. 4. (Color online) Network of leaky IF neurons: (a) Fano factor and (b) correlation time as functions of synaptic coupling strength with different values of the leak parameter ( $\gamma = 0.1, 1$ ) and refractory period ( $\tau_{\text{ref}} = 0, 2, 4$  ms) from network simulations (solid lines) and iterative scheme (dashed lines). Arrows indicate the critical coupling according to Eq. (8).

coupling strength [Fig. 4(b)]. In the supercritical case with the standard value of leak ( $\gamma = 1$ ) the correlation time attains values of a few tens of ms, which is an order of magnitude larger than the mean interspike interval (ISI) of the single cell, i.e., the time scale of the fast units the network is made of. Hence, although modified quantitatively, the mechanism for the emergence of slow fluctuations in networks of LIF neurons is the self-consistent amplification of low-frequency noise.

This view is supported by the following estimation of the critical value of the coupling. A linear map similar to Eq. (4) exists for IF neurons in the mean-driven regime [19] that holds true for *intermediate* noise levels [28]:

$$S_{xx,n+1}(0) = J^2 r_0^2 (C_E + g^2 C_I) \tilde{Z}^2(0) S_{xx,n}(0). \quad (7)$$

Here,  $\tilde{Z}(f) = r_0 \int_0^{1/r_0} dt Z(t) e^{2\pi i f t}$  is the Fourier transform of the neuron's infinitesimal phase response curve (PRC) [29]. For the perfect IF model,  $Z(t)$  is just a constant and Eq. (7) reduces to Eq. (4). For the leaky IF model, we have  $Z(t) = \theta(t - \tau_{\text{ref}}) \exp[\gamma(t - \tau_{\text{ref}})/\tau_m] / (\mu - \gamma v_R/\tau_m)$  with  $\mu = R I_{\text{ext}}/\tau_m + J r_0 (C_E - g C_I)$  and  $r_0 = [\tau_{\text{ref}} + \frac{\tau_m}{\gamma} \ln(\frac{\mu \tau_m - \gamma v_R}{\mu \tau_m - \gamma v_T})]^{-1}$ . Both at very regular and very irregular inputs the linear map for  $S_{xx}(0)$  is not valid anymore but has to be replaced by the full functional map, leading to finite fixed points of the Fano factor for both weak and strong coupling. However, the map above still allows for an estimation of the critical coupling strength for our perfectly balanced case ( $g = C_E/C_I = 4$ ), yielding

$$J_c = (r_0 \tilde{Z}(0) C_E \sqrt{C_E^{-1} + C_I^{-1}})^{-1}. \quad (8)$$

Inspection of this formula reveals a surprisingly moderate effect of the choice of  $\gamma$  on this critical value but a considerable change if the refractory period  $\tau_{\text{ref}}$  is varied. The theoretically predicted shifts of  $J_c$  to substantially larger values by increasing  $\tau_{\text{ref}}$  from 0 to 2 or 4 ms are confirmed in our network simulations and by the iterative scheme [cf. arrows in Fig. 4(a)].

**Conclusions.** Our results show that arbitrarily slow time scales can emerge in the fluctuations of a sparsely connected random network of spiking neurons if the synaptic coupling exceeds a critical value. The transition from low to high Fano factor can be understood in a network of perfect IF neurons, in which the self-consistent connection between the

low-frequency variability of the input spikes to a neuron and the low-frequency variability of its output spikes attains the simple form of a linear map. This map becomes unstable at the critical coupling and, hence, for stronger coupling, the spectral power at low frequencies—or, equivalently, the asymptotic Fano factor—grows without bound if time windows and the system size are enlarged. Remarkably, close to the critical value, the time scale of the system attains a *minimum*.

Measured Fano factors and correlation times change quantitatively, but the main effects reported survive if we use a network of leaky integrate-and-fire neurons with nonvanishing absolute refractory period and transmission delays. We are confident that the effect explained in a simple way for a network of perfect IF models is the same as reported recently by Ostojic [14]. It might be that our findings are also relevant for explaining slow fluctuations in networks with clustered connections [12], in which clustering may lower the value of the critical coupling constant. We note that the “heterogeneity of firing rates,” i.e., the broad spike-count distribution for time windows extending over several ISIs observed in Ref. [14], is just a consequence of the slow temporal fluctuations in the single neuron's spiking and of the independence of neurons in the network. This view is underpinned by the quantitative agreement of rate histograms in network simulations and the iterative scheme (not shown), where the latter solely uses the self-consistency condition in a single-neuron setup. Further support comes from the correct prediction of the critical coupling when varying the leak term and the refractory period of the neuron.

We finally note that the slow fluctuations are in part based on large deviations towards negative membrane voltage. This is in line with recent observations in the fluctuation-dominated regime of the considered networks [13] and is a rather unphysiological feature of the model. It remains to be seen whether networks of IF neurons with conductance-based instead of current-based synapses can display similar slow fluctuations as were observed here.

B.L. would like to thank Alexander Neiman for a fruitful discussion. This work has been funded by the BMBF (FKZ: 01GQ1001A) and by the European Research Council under Grant Agreement No. 268689 (MultiRules).

- 
- [1] M. Mezard, G. Parisi, and M. Virasoro, *Spin Glass Theory and Beyond* (World Scientific, Singapore, 1987).
  - [2] P. Dutta and P. M. Horn, *Rev. Mod. Phys.* **53**, 497 (1981).
  - [3] N. Brunel and X. J. Wang, *J. Comput. Neurosci.* **11**, 63 (2001).
  - [4] G. Mongillo, O. Barak, and M. Tsodyks, *Science* **319**, 1543 (2008).
  - [5] S. Lim and M. S. Goldman, *Nat. Neurosci.* **16**, 1306 (2013).
  - [6] K.-F. Wong and X.-J. Wang, *J. Neurosci.* **26**, 1314 (2006).
  - [7] D. Durstewitz and G. Deco, *Eur. J. Neurosci.* **27**, 217 (2008).
  - [8] H. Sompolinsky, A. Crisanti, and H. J. Sommers, *Phys. Rev. Lett.* **61**, 259 (1988).
  - [9] I. Ginzburg and H. Sompolinsky, in *Advances in Neural Information Processing Systems*, edited by J. Cowan, G. Tesoro, and J. Alsppector (Morgan Kaufmann Publishers, San Francisco, 1994), Vol. 6, p. 471.
  - [10] A. Zumdieck, M. Timme, T. Geisel, and F. Wolf, *Phys. Rev. Lett.* **93**, 244103 (2004).
  - [11] R. Zillmer, N. Brunel, and D. Hansel, *Phys. Rev. E* **79**, 031909 (2009).
  - [12] A. Litwin-Kumar and B. Doiron, *Nat. Neurosci.* **15**, 1498 (2012).
  - [13] B. Kriener, H. Enger, T. Tetzlaff, H. E. Plesser, M.-O. Gewaltig, and G. T. Einevoll, *Front. Comput. Neurosci.* **8**, 136 (2014).
  - [14] S. Ostojic, *Nat. Neurosci.* **17**, 594 (2014).
  - [15] J. Aljadeff, M. Stern, and T. Sharpee, *Phys. Rev. Lett.* **114**, 088101 (2015).
  - [16] See the comment by R. Engelken, F. Farkhooi, D. Hansel, C. van Vreeswijk, and F. Wolf, doi:10.1101/017798 (2015) and the response to the comment by S. Ostojic, doi:10.1101/020354 (2015).

- [17] L. F. Abbott and C. van Vreeswijk, *Phys. Rev. E* **48**, 1483 (1993).
- [18] N. Brunel, *J. Comput. Neurosci.* **8**, 183 (2000).
- [19] T. Schwalger, F. Droste, and B. Lindner, *J. Comput. Neurosci.* **39**, 29 (2015).
- [20] A. Lerchner, C. Ursta, J. Hertz, M. Ahmadi, P. Ruffiot, and S. Enemark, *Neural Comput.* **18**, 634 (2006).
- [21] B. Dummer, S. Wieland, and B. Lindner, *Front. Comput. Neurosci.* **8**, 104 (2014).
- [22]  $S_{xx}(0)$  is determined by the asymptotic long-time spike-count variance that is proportional to the variance of the freely evolving process  $v_{\text{free}}(t)$  according to Eq. (3) with  $\gamma = 0$  but without applying the reset. The growth of the variance of  $v_{\text{free}}(t)$  in time is determined by the diffusion coefficient which is related via the Kubo relation to the power spectrum of the motion's velocity at zero frequency, and hence with the noise spectrum  $S_{\eta\eta}(0)$ .
- [23] M. Spiridon and W. Gerstner, *Network: Comput. Neural. Syst.* **10**, 257 (1999).
- [24] M. Mattia and P. Del Giudice, *Phys. Rev. E* **66**, 051917 (2002).
- [25] According to Ref. [30],  $S_{xx}(0) = r_0 C_v^2 [1 + 2 \sum_{k=1}^{\infty} \rho_k]$ , where  $C_v$  is the coefficient of variation of the interspike intervals (ISIs),  $I_i = t_i - t_{i-1}$ , and  $\rho_k$  is the serial correlation coefficient among ISIs that are lagged by an integer  $k$ . For a fixed firing rate  $r_0$ , the spectrum can vanish if  $C_v = 0$  (completely regular spike train) or for  $\sum_{k=1}^{\infty} \rho_k = -1/2$  (perfectly anticorrelated ISIs). Our simulations indicate the latter.
- [26] W. Bair, C. Koch, W. Newsome, and K. Britten, *J. Neurosci.* **14**, 2870 (1994).
- [27] A. B. Neiman, T. A. Yakusheva, and D. F. Russell, *J. Neurophysiol.* **98**, 2795 (2007).
- [28] More precisely, a linear map holds approximately if  $S_{xx,n}(0) \tilde{Z}^2(0) \gg 2 \sum_{k=1}^{\infty} S_{xx,n}(kr_0) |\tilde{Z}(kr_0)|^2$ .
- [29] G. B. Ermentrout and D. H. Terman, *Mathematical Foundations of Neuroscience* (Springer, Berlin, 2010).
- [30] D. R. Cox and P. A. W. Lewis, *The Statistical Analysis of Series of Events* (Chapman and Hall, London, 1966).